

LUMINOSITY- AND MORPHOLOGY-DEPENDENT CLUSTERING OF GALAXIES

CLAUS BEISBART¹ AND MARTIN KERSCHER^{2,1}*July 26, 2000 accepted in the ApJ*

ABSTRACT

How does the clustering of galaxies depend on their inner properties like morphological type and luminosity? We address this question in the mathematical framework of marked point processes and clarify the notion of luminosity and morphological segregation. A number of test quantities such as conditional mark-weighted two-point correlation functions are introduced. These descriptors allow for a scale-dependent analysis of luminosity and morphology segregation. Moreover, they break the degeneracy between an inhomogeneous fractal point set and actual present luminosity segregation.

Using the Southern Sky Redshift Survey 2 (da Costa et al. 1998, SSRS2) we find both luminosity and morphological segregation at a high level of significance, confirming claims by previous works using these data (Benoist et al. 1996; Willmer et al. 1998). Specifically, the average luminosity and the fluctuations in the luminosity of pairs of galaxies are enhanced out to separations of $15h^{-1}$ Mpc. On scales smaller than $3h^{-1}$ Mpc the luminosities on galaxy pairs show a tight correlation. A comparison with the random-field model indicates that galaxy luminosities depend on the spatial distribution and galaxy-galaxy interactions. Early-type galaxies are also more strongly correlated, indicating morphological segregation. The galaxies in the PSCz catalog (Saunders et al. 2000) do not show significant luminosity segregation. This again illustrates that mainly early-type galaxies contribute to luminosity segregation. However, based on several independent investigations we show that the observed luminosity segregation can not be explained by the morphology-density relation alone.

Subject headings: methods: statistical – large-scale structure of universe – galaxies: clusters – galaxies: fundamental parameters (classification, luminosities)

1. INTRODUCTION

The geometrical properties of the large-scale structure in the Universe are a common test for cosmic structure formation theories. However, comparisons between analytical models and observational data suffer from the fact, that theoretical predictions refer to mass correlations whereas in galaxy catalogs only luminous matter is observed. This gap gives rise to the bias problem and is usually filled using biasing schemes. Mostly, these schemes relate properties of the density contrast field to the distribution of the galaxies, thus combining descriptors of a random field with point process characteristics. Due to the nature of the *dark* matter, only indirect methods are feasible to address the bias problem empirically. In this line of thought, it seems promising to ask whether the clustering properties of galaxies depend on their mass, luminosity or morphological type. The idea behind this search for *luminosity and morphology segregation* is that different galaxy subpopulations may trace the dark matter distribution on a different level.

Empirical investigations concerned with this problem were mainly carried out in two directions:

- The two-point correlation function was calculated for a series of volume-limited subsamples from galaxy surveys. A difference in the amplitude of the two-correlation function between such samples was interpreted as an indication of luminosity or morphology-segregation. For luminosity segregation see e.g., Ostriker & Turner (1979); Hamilton (1988); Domínguez-Tenreiro & Martínez (1989); Benoist et al. (1996); Willmer et al. (1998). The void probability and cross-correlation functions have been used by Maurogordato & Lachièze-Rey (1987) and Valotto & Lambas (1997). For morphology segregation see e.g., Domínguez-Tenreiro et al. (1994); Hermit et al. (1996). These investigations are sensitive to segregation effects on scales roughly between 1 and $10h^{-1}$ Mpc. However, Coleman & Pietronero (1992) gave an alternative explanation of the rising amplitude in terms of a fractal galaxy distribution, without any luminosity-dependent clustering.
- Dressler (1980) showed that in clusters of galaxies the morphological type of a galaxy is depending on the local (surface) density; this is called the morphology-density relation. For mainly spherical clusters, where the local density is closely related to the radial distance from the cluster center, this translates into the Butcher & Oemler (1978) effect. For more recent accounts of the morphology-density relation see Caon & Einasto (1995); Dressler et al. (1997); Andreon et al. (1997). Most of these investigations focussed on the morphology-density relation *inside* clusters, hence on scales smaller than $1.5h^{-1}$ Mpc. But the morphology-density relation can be observed also in groups of galaxies (Postman & Geller 1984; Maia & da Costa 1990) and for dwarf galaxies in the field (Binggeli et al. 1990).

¹Sektion Physik, Ludwig-Maximilians-Universität, Theresienstraße 37, 80333 München, Germany, email: beisbart@theorie.physik.uni-muenchen.de

²Department of Physics and Astronomy, The Johns Hopkins University, Baltimore, MD 21218, email: kerscher@pha.jhu.edu

With the first method, one compares two-point correlation functions, whereas with the second, one considers the relation between the local number density and the local morphology, i.e., a comparison of one-point densities. Both methods rely on unweighted descriptors.

The observations of luminosity segregation or the morphology–density relation were complemented by theoretical considerations. Motivated by the offset between the galaxy–galaxy and the cluster–cluster correlation functions, Kaiser (1984) and Bardeen et al. (1986) suggested that clusters may be understood as peaks in the density field. Starting from a Gaussian random field they showed how the amplitude of the correlation function increases with the threshold imposed on the initial density field, i.e., with the height of the peaks in the density field. This also provided an explanation for the morphology–density relation (Evrard et al. 1990).

Other authors developed a conceptual framework to describe the bias (see e.g., Coles 1993, Dekel & Lahav 1999, and refs. therein). Within these biasing schemes, characteristics of the galaxy point pattern are connected with descriptions of the density field – often the mass density contrast and the galaxy over-density are compared. The relation is assumed to be (non-) linear and either deterministic or stochastic (Dekel & Lahav 1999). More involved biasing schemes were considered to facilitate the extraction of reasonable galaxy catalogs from N -body simulations (see e.g., Kates et al. 1991, Weiß & Buchert 1993, Kauffmann et al. 1997).

In this paper, we introduce a new method to handle the bias problem. Our approach complements both the more observational methods and the analytical and theoretical treatments. We understand the galaxies with their intrinsic properties as a realization of a marked point process. Using conditional weighted correlation functions, we put an intermediate step in between the pure point process statistics and the statistics of random fields. In our description stochasticity is present from the very beginning. It provides us with stochastic models which enable us to exclude certain families of models for the luminosity distribution of galaxies.

More precisely, the aim of our paper is twofold:

On the one hand, we want to clarify the notion of luminosity/morphology–dependent clustering by discussing this task in the mathematical framework of marked point processes (Sect. 2). This allows us to introduce a new class of indicators sensitive to luminosity segregation (Subsect. 3.1) and to discuss models for marked point patterns (Subsect. 3.2 and Subsect. 6.1). Methods similar in spirit are the cross-correlation function and luminosity-weighted correlation functions considered by Alimi et al. (1988), Börner et al. (1989), Valls-Gabaud et al. (1989), and Tegmark & Bromley (1999). Our methods allow for a study of the interplay between the spatial clustering and the luminosity and morphology distribution of the galaxies, complementing the characterization of the purely spatial distribution of the galaxies.

On the other hand, we address the empirical question, whether the luminosities or morphological types of galaxies depend on their spatial distribution by analyzing the SSRS2 catalog (da Costa et al. 1998) in Sect. 4. Our results show a significant scale-dependent luminosity and morphological segregation. To understand the data more closely we compare our results with the random field model. The comparison with galaxy samples from the IRAS 1.2Jy (Fisher et al. 1995) and the PSCz (Saunders et al. 2000) strengthens our conclusions.

In Sect. 5 we will discuss the usual way of looking for luminosity segregation via the amplitude of the correlation function in the framework of marked point processes. The criticism by Coleman & Pietronero (1992) is reviewed and we show that this degeneracy between a fractal spatial distribution and luminosity segregation is not encountered if one uses the mark–correlation functions we proposed. This strengthens the conclusions of our empirical work in Sect. 4.

Investigations inside clusters of galaxies gave clear evidence for the morphology–density relation (Dressler 1980). In Sect. 6 we however show that the observed luminosity segregation may not be explained by the spatial interaction of early- and late-type galaxies *alone*. Luminosity segregation is already present in the subsample consisting only of early-type galaxies.

In Sect. 7 we summarize and provide an outlook. Technicalities concerning the estimation of mark–correlation functions are left to Appendix A.

2. MARKED POINT DISTRIBUTIONS

Consider a set of points $X = \{\mathbf{x}_i\}_{i=1}^N$ given by the spatial coordinates $\mathbf{x}_i \in \mathbb{R}^3$ of the galaxies inside a sample geometry \mathcal{D} . Additionally to their positions in space we know intrinsic properties of the galaxies like their luminosity, mass, morphological type etc. Formally, we assign to each point \mathbf{x}_i a mark m_i , e.g., the luminosity of the galaxy $m_i = L_i$, and obtain the marked point set $X^M = \{(\mathbf{x}_i, m_i)\}_{i=1}^N$. We are not limited to continuous marks like the luminosity, also discrete marks like morphological types (e.g., *spiral* or *elliptical*) can be used. The description of the galaxy distribution in a *statistical* way that we will propose in this article, rests on the assumption that the empirical data points may be considered as a realization of a marked point process. Formally, $X = \{\mathbf{x}_i\}_{i=1}^N$ and $M = \{m_i\}_{i=1}^N$ may be thought of as realizations of a point process each, which may be characterized by the usual point process statistics. Physically, however, we are interested in the interplay between the spatial statistics and the mark distribution, which is expressed in quantities combining information on the space and the mark distribution.

The second-order theory of marked point processes was developed in detail by Stoyan (1984) where also a mark-weighted conditional correlation function was introduced (see also Stoyan & Stoyan 1994). Some aspects have been also discussed by Peebles (1980).

2.1. One-point properties

A point process may be characterized by its moments. For a homogeneous spatial point distribution the first moment is the mean number density ρ , which may be estimated with $N/|\mathcal{D}|$, where $|\mathcal{D}|$ is the volume of the sample and N the number

of points inside \mathcal{D} . Let $\rho_1^M(m)dm$ denote the probability that the value of a mark lies within the interval $[m, m + dm]$, then the mean mark \bar{m} and the variance of the marks V are given by

$$\bar{m} = \int dm \rho_1^M(m)m, \quad \text{and} \quad V = \int dm \rho_1^M(m)(m - \bar{m})^2, \quad (1)$$

which may be estimated by

$$\frac{1}{N} \sum_{i=1}^N m_i \quad \text{and} \quad \frac{1}{N-1} \left(\sum_{i=1}^N m_i^2 - N\bar{m}^2 \right),$$

respectively.

For a homogeneous marked point process, the joint probability $\rho_1^{SM}(\mathbf{x}, m)dVdm$ of finding³ a point at position \mathbf{x} with mark m , splits into a space-independent mark probability and the constant mean density: $\rho_1^M(m)dm \times \rho dV$. In general, the mark distribution ρ_1^M is not homogeneous. Note that this notion of independence does not rule out luminosity segregation at all and seems a physically justified assumption, since it simply requires that no region of space has an a priori specified mark distribution different from that one of another region.

2.2. Two-point properties

The second-order properties of the spatial distribution of the point set X are fully specified by the product-density $\rho_2^S(\mathbf{x}_1, \mathbf{x}_2)dV_1dV_2$ giving the probability of finding a point at \mathbf{x}_1 and another point at \mathbf{x}_2 . For a stationary and isotropic point distribution we have with $r = |\mathbf{x}_1 - \mathbf{x}_2|$

$$\rho_2^S(\mathbf{x}_1, \mathbf{x}_2) = \rho^2(1 + \xi(r)) \quad (2)$$

with the two-point correlation function $\xi(r)$. Similarly, second-order properties of the marked point set X^M are fully specified by the mark product-density:

$$\rho_2^{SM}((\mathbf{x}_1, m_1), (\mathbf{x}_2, m_2)) dV_1dm_1 dV_2dm_2 \quad (3)$$

is the joint probability of finding a galaxy at \mathbf{x}_1 with the mark m_1 and another point at \mathbf{x}_2 with the mark m_2 . Hence the (spatial) product-density $\rho_2^S(\mathbf{x}_1, \mathbf{x}_2)$ is the marginal density

$$\rho_2^S(\mathbf{x}_1, \mathbf{x}_2) = \int dm_1 \int dm_2 \rho_2^{SM}((\mathbf{x}_1, m_1), (\mathbf{x}_2, m_2)). \quad (4)$$

With an appropriate chosen integration measure similar definitions apply for discrete marks.

Now consider a finite domain \mathcal{D} . The normalization of ρ_2^S is given by

$$\mathcal{N}_2 = \int_{\mathcal{D}} dx_1^3 \int_{\mathcal{D}} dx_2^3 \rho_2^S(\mathbf{x}_1, \mathbf{x}_2) = \mathbb{E}[N(N-1)], \quad (5)$$

with N the number of points of one realization inside \mathcal{D} , and \mathbb{E} the mean value over several realizations.

Respecting this normalization, a marginal product density for the marks can be defined by

$$\rho_2^M(m_1, m_2) = \frac{1}{\mathcal{N}_2} \int_{\mathcal{D}} dx_1^3 \int_{\mathcal{D}} dx_2^3 \rho_2^{SM}((\mathbf{x}_1, m_1), (\mathbf{x}_2, m_2)). \quad (6)$$

$\rho_2^M(m_1, m_2)dm_1dm_2$ quantifies the probability to find the marks m_1 and m_2 at two given points in the distribution. Mathematically, $\rho_2^M(m_1, m_2)$ quantifies a real two-point property. Physically, however, we expect – at least in our case – that intrinsic correlations in mark space are not present, i.e., that

$$\rho_2^M(m_1, m_2) = \rho_1^M(m_1)\rho_1^M(m_2). \quad (7)$$

Otherwise the probability of finding a galaxy with mark m_i in a fixed sample would depend on the other marks regardless how distant they are, a consequence which may seem reasonable in biosciences (epidemiology) but not in our case of large galaxy surveys. In other words, *spatial* mark correlations may be present, but *globally* the presence of a mark with value m in the sample does not prearrange the values of the other marks. Typically, the one-point mark distribution ρ_1^M is inhomogeneous in mark-space. Therefore, one cannot check the relation (7) from one realization only; several independent samples are needed. In future redshift surveys it may be possible to extract approximately independent subsamples separated by a large distance, allowing for such a check. Throughout this paper, we will adopt the assumption (7).

2.3. Mark correlations depending on the spatial distance

In the following we want to know, whether the clustering in space and the luminosity distribution are correlated. We define the conditional mark density:

$$\mathcal{M}_2(m_1, m_2 | \mathbf{x}_1, \mathbf{x}_2) = \begin{cases} \frac{\rho_2^{SM}((\mathbf{x}_1, m_1), (\mathbf{x}_2, m_2))}{\rho_2^S(\mathbf{x}_1, \mathbf{x}_2)} & \text{for } \rho_2(\mathbf{x}_1, \mathbf{x}_2) \neq 0, \\ 0 & \text{otherwise.} \end{cases} \quad (8)$$

³For the sequel we speak for reasons of simplicity of “finding at \mathbf{x} with mark m ” instead of “finding in a volume element dV at position \mathbf{x} with mark in the range $[m, m + dm]$ ”.

For a stationary and isotropic point distribution, $\mathcal{M}_2(m_1, m_2 | \mathbf{x}_1, \mathbf{x}_2)$ is the probability density⁴ of finding the marks m_1 and m_2 at two galaxies located at \mathbf{x}_1 and \mathbf{x}_2 , respectively, under the condition that galaxies at these positions are present in the data. For the following, we assume that this quantity is only a function of the galaxy distance $r = |\mathbf{x}_1 - \mathbf{x}_2|$: $\mathcal{M}_2(m_1, m_2 | r)$. This assumption expresses a sort of homogeneity and isotropy, however, it does not presuppose a well-defined mean density and is thus only a weak requirement.

The full mark product-density can be written as

$$\rho_2^{SM}((\mathbf{x}_1, m_1), (\mathbf{x}_2, m_2)) = \mathcal{M}_2(m_1, m_2 | \mathbf{x}_1, \mathbf{x}_2) \rho_2^S(\mathbf{x}_1, \mathbf{x}_2). \quad (9)$$

$\mathcal{M}_2(m_1, m_2 | r)$ is a function depending on three variables and is therefore hard to estimate. With the mark-weighted correlation functions and the discrete mark-correlation function we further distill the information as discussed in Subsection 3.1.

If the distribution of the marks is *independent* of the distribution of the points, the conditional mark density becomes independent of r :

$$\mathcal{M}_2(m_1, m_2 | r) = \rho_1^M(m_1) \rho_1^M(m_2), \quad (10)$$

Intuitively, this independence may be understood in the following way: After having distributed galaxies in space, we choose marks (as a realization of a second independent stochastic process) and distribute them randomly without any regard to the clustering of the galaxies.

Equation (10) is the basic assumption behind projection formulas like Limber's equation (Peebles 1980). If, on the other hand, $\mathcal{M}_2(m_1, m_2 | r)$ does depend on r , we speak of e.g., *mark segregation*: The probability of observing two marks m_1 and m_2 (e.g., luminosities) on the galaxies at \mathbf{x}_1 and \mathbf{x}_2 varies with the separation r of these two galaxies.

Note, that for every empirical dataset of marked points (which we may think of as realization of a marked point process) we can artificially construct another dataset with the same spatial features showing no mark segregation by redistributing the marks to the points randomly. This bootstrap resampling strategy for the marks provides a method for testing the statistical significance of mark correlations.

2.4. Spatial correlations depending on the marks

There are complementary definitions of this sort of independence or luminosity segregation. For example, we can think the other way round and define a conditional density that there be two galaxies at \mathbf{x}_1 and \mathbf{x}_2 , under the condition that their marks be m_1 and m_2 :

$$\mathcal{S}_2(\mathbf{x}_1, \mathbf{x}_2 | m_1, m_2) = \begin{cases} \frac{\rho_2^{SM}((\mathbf{x}_1, m_1), (\mathbf{x}_2, m_2)) / \mathcal{N}_2}{\rho_2^M(m_1, m_2)} & \text{for } \mathcal{N}_2 \rho_2^M(m_1, m_2) \neq 0, \\ 0 & \text{otherwise,} \end{cases} \quad (11)$$

with \mathcal{N}_2 given in Eq. (5). If the conditional space correlation is independent of m_1 and m_2 , then $\mathcal{S}_2(\mathbf{x}_1, \mathbf{x}_2 | m_1, m_2) = \rho_2^S(\mathbf{x}_1, \mathbf{x}_2) / \mathcal{N}_2$. In the case of luminosity segregation, on the other hand, the values of the marks influence the spatial clustering. Using \mathcal{S}_2 we will discuss the usual way of looking for luminosity segregation in Subsect. 5.1.

2.5. n -point properties

For completeness we mention that n -point-properties may be discussed in the same way. Basic quantities are the n -point product densities $\rho_n^{SM}((\mathbf{x}_1, m_1), \dots, (\mathbf{x}_n, m_n))$ and the conditional densities $\mathcal{M}_n(m_1, \dots, m_n | \mathbf{x}_1, \dots, \mathbf{x}_n)$. At this level the issue may be re-discussed, whether the mark distribution depends on the spatial clustering.

Robust statistics for the clustering of galaxies in space, incorporating higher-order correlations, are the J -function (van Lieshout & Baddeley 1996, Kerscher 1998, Kerscher et al. 1999) and the Minkowski functionals (Mecke et al. 1994, for a review see Kerscher 2000). A first extension of the J -functions to discretely marked point sets is discussed by van Lieshout & Baddeley (1997). The application to galaxy catalogs and the generalization for continuous marks is currently under investigation.

3. MARK-WEIGHTED CONDITIONAL CORRELATION FUNCTIONS AND MODELS FOR MARKED POINT DISTRIBUTIONS

Since the joint space and mark product-density ρ_2^{SM} and the conditional mark density \mathcal{M}_2 depend on three variables at least, they are not easy to handle. Therefore, we discuss quantities accessible both to straight-forward interpretation and to numerical estimation. Particularly, we investigate the mark-weighted conditional densities.

3.1. Mark-weighted conditional correlation functions

For a non-negative weighting function $f(m_1, m_2)$ we define the average over pairs with separation r :

$$\langle f \rangle_P(r) = \int dm_1 \int dm_2 f(m_1, m_2) \mathcal{M}_2(m_1, m_2 | r). \quad (12)$$

$\langle f \rangle_P(r)$ is the expectation value of the weighting function f (depending only on the marks), under the condition that we find a galaxy-pair with separation r in the data. With this definition we separate the mark correlation properties from the spatial clustering properties of the underlying point-distribution, as can be seen directly from

$$\langle f \rangle_P(r) = \frac{\int dm_1 \int dm_2 f(m_1, m_2) \rho_2^{SM}((\mathbf{x}_1, m_1), (\mathbf{x}_2, m_2))}{\rho_2^S(r)} \quad (13)$$

for $\rho_2^S(r) \neq 0$. We are free to choose appropriate weighting functions adopted to our problem. In the following we discuss common choices from the literature and introduce some new ones.

⁴The notation $\mathcal{M}_2(m_1, m_2 | r)$ is somehow imprecise, since it does not remind us of the fact that the marks refer to given points \mathbf{x}_1 and \mathbf{x}_2 . For simplicity, we do not use a more accurate notation like $\mathcal{M}_2(m_1(\mathbf{x}_1), m_2(\mathbf{x}_2) | r)$.

3.1.1. *Continuous marks*

Using several positive weighting functions we construct statistical indicators to investigate the mark correlation properties of a point set (see also Stoyan & Stoyan 1994 and Schlather 1999, we assume that the marks are positive numbers):

1. At first we consider the mean mark:

$$k_m(r) = \frac{\langle m_1 + m_2 \rangle_{\mathbf{P}}(r)}{2 \bar{m}}. \quad (14)$$

k_m equal unity indicates the absence of mark segregation. A preferred clustering of marks e.g., $m > \bar{m}$ at a scale r can be concluded from $k_m(r) > 1$.

2. Closely related is Stoyan's k_{mm} -function⁵ (Stoyan & Stoyan 1994):

$$k_{mm}(r) = \frac{\langle m_1 m_2 \rangle_{\mathbf{P}}(r)}{\bar{m}^2}. \quad (15)$$

With k_{mm} we investigate the square of the geometric mean of the marks on points at a distance of r . Therefore, a preferred clustering of marks at a scale r can be inferred from $k_{mm}(r) > 1$ similar to k_m . Note that if the mark is the mass of a galaxy, k_{mm} may serve as an estimator for the conditional mass correlations $\mathbb{E}[\varrho(0)\varrho(\mathbf{x})]/\varrho_2^2(0, \mathbf{x})$, where $\varrho(\mathbf{x})$ is the mass-density at position \mathbf{x} , thus it quantifies the ratio between galaxy and mass correlations.

3. The mark variogram (Walder & Stoyan 1996) is defined by

$$\gamma(r) = \left\langle \frac{1}{2}(m_1 - m_2)^2 \right\rangle_{\mathbf{P}}(r) = \langle m_1^2 \rangle_{\mathbf{P}}(r) - \langle m_1 m_2 \rangle_{\mathbf{P}}(r). \quad (16)$$

$\gamma(r)$ equals the variance V of the mark distribution, if mark segregation is absent; it exceeds V at some scale r , if points that are about r apart from each other, tend to have very different marks.

4. Another tool for investigating the variance of the mark distribution is the mark covariance function (Cressie 1991)

$$cov(r) = \langle m_1 m_2 \rangle_{\mathbf{P}}(r) - \langle m_1 \rangle_{\mathbf{P}}(r) \langle m_2 \rangle_{\mathbf{P}}(r) = \langle m_1 m_2 \rangle_{\mathbf{P}}(r) - \langle m_1 \rangle_{\mathbf{P}}^2(r). \quad (17)$$

Thus, luminosity segregation can be detected by looking whether $cov(r)$ does significantly differ from zero for some r .

5. Both $\gamma(r)$ and $cov(r)$ mix the two-point and one-point fluctuations of the mark distribution. To quantify the fluctuations of the mark at one point only, given there is another point at distance r , we suggest to use

$$var(r) = \left\langle (m_1 - \langle m_1 \rangle_{\mathbf{P}}(r))^2 \right\rangle_{\mathbf{P}}(r). \quad (18)$$

From Eq. (16) and (17) one directly obtains

$$var(r) = \gamma(r) + cov(r). \quad (19)$$

6. Closely related to $cov(r)$ is the mark-correlation function of Isham (1985)

$$cor(r) = \frac{\langle m_1 m_2 \rangle_{\mathbf{P}}(r) - \langle m_1 \rangle_{\mathbf{P}}^2(r)}{\langle m_1^2 \rangle_{\mathbf{P}}(r) - \langle m_1 \rangle_{\mathbf{P}}^2(r)} = \frac{cov(r)}{var(r)}, \quad (20)$$

the covariance function divided by the fluctuations of the mark.

Schlather (1999) showed that there is an ambiguity in the definitions of these mark characteristics at r equal zero, but there is no problem for $r > 0$. Since we always have to use a finite and non-zero r to estimate these mark characteristics, this ambiguity is a technical point we do not need to consider further. As another characteristic for marked point distributions, Capobianco & Renshaw (1998) consider the extension of the k_{mm} function on a two-dimensional grid.

3.1.2. *Discrete marks*

To investigate the correlation properties between galaxies of different morphological types the marks m_i are chosen out of a finite range of attributes $m_i \in \{t_\alpha\}_{\alpha=1}^A$. We also could use other intrinsic properties, like spectral features etc. of the galaxies to define these discrete marks. Similarly, a finite binning may be used for continuous marks. Consider pairwise disjoint bins I_α in luminosity space, then the mark is chosen to be $m_i = t_\alpha$ if the luminosity of the galaxy is $L_i \in I_\alpha$.

For discrete marks the following symmetric weight functions for $\alpha, \beta = 1, \dots, A$ are appropriate:

$$f_{t_\alpha t_\beta}(m_1, m_2) = \delta_{m_1 t_\alpha} \delta_{m_2 t_\beta} + (1 - \delta_{\alpha\beta}) \delta_{m_2 t_\alpha} \delta_{m_1 t_\beta}, \quad (21)$$

where the Kronecker $\delta_{m_1 t_\alpha}$ equals unity if $m_1 = t_\alpha$ and zero otherwise. According to Eq. (12) we consider the (normalized) conditional cross-correlation functions

$$C_{t_\alpha, t_\beta}(r) = \langle f_{t_\alpha t_\beta} \rangle_{\mathbf{P}}(r). \quad (22)$$

⁵Also called (normalized) mark-correlation function, see however the comments by Schlather (1999).

Clearly, $\sum_{\alpha=1}^A \sum_{\beta=\alpha}^A f_{t_\alpha, t_\beta} = 1$ and therefore also

$$\sum_{\alpha=1}^A \sum_{\beta=\alpha}^A C_{t_\alpha, t_\beta}(r) = 1 \quad (23)$$

for all r . If the marks are independent on the distribution in space one can show that

$$C_{t_\alpha, t_\beta}(r) = \frac{2 \rho_{t_\alpha} \rho_{t_\beta}}{\rho^2} \quad \text{for } t_\alpha \neq t_\beta, \quad \text{and} \quad C_{t_\alpha, t_\alpha}(r) = \frac{\rho_{t_\alpha}^2}{\rho^2}, \quad (24)$$

with the number density ρ_{t_α} of points with mark t_α .

Summarizing, there is a variety of test quantities which allows us to search for luminosity segregation in real data. Note that these quantities are applicable to a single data set without the need of constructing a series of volume-limited subsamples. With these methods we are able to gain new insights into the luminosity and morphological dependent clustering of galaxies (Sect. 4). As we will show in Subsect. 5.3, these methods break the degeneracy between fractal spatial structure and luminosity segregation.

3.2. Marked Poisson processes

Before applying these test quantities to real data we explain their properties with a simple model, where the marks are artificially constructed from the spatial pattern. Other models are discussed in Subsect. 4.2 and Subsect. 6.1.

We start with Poisson-distributed points \mathbf{x}_i , with number density ρ and assign to each point the mark $m_i = N_i(R)$, where $N_i(R)$ is the number of other points within a sphere of radius R around the point \mathbf{x}_i . Explicit formulas for $\gamma(r)$ and $k_{mm}(r)$ were derived by Walder & Stoyan (1996). In Fig. 1 we compare numerical simulations with the theoretical curves. Points, which are members of a pair with small separation, are on average situated in over-dense regions, have more neighbors and therefore get higher marks. This is reflected by $k_m(r)$ and $k_{mm}(r)$ larger than unity on small scales ($k_m(r)$ and $k_{mm}(r)$ indeed show a jump at $r = R$). Since nearby points get similar marks, the mark variogram is suppressed on small scales, which can be seen directly from the reduced $\gamma(r)$ on small scales. However, the mean fluctuations of the mark at one point are not influenced by the presence of nearby other points for a Poisson process, and consequently $\text{var}(r) = V$. The strong correlation of marks on small scales can be seen also from the the covariance $\text{cov}(r)$ and correlation $\text{cor}(r)$. Empirically, both $\text{cov}(r)$ and $\text{cor}(r)$ and also $k_m(r)$ and $k_{mm}(r)$ exhibit the same information content. We also found this in our analysis of the galaxy catalogs in Sect. 4. Moreover, $\gamma(r)$ may be expressed with $\text{cov}(r)$ and $\text{var}(r)$ (Eq. (19)). Therefore, we will focus in the following only on $k_{mm}(r)$, $\text{var}(r)$ and $\text{cov}(r)$.

4. LUMINOSITY AND MORPHOLOGICAL SEGREGATION IN THE GALAXY DISTRIBUTION

Having clarified the basic notion of luminosity segregation, we now apply the above-defined characteristics to real data and discuss the empirical question whether there is evidence for luminosity segregation in the large-scale structure of the galaxy distribution. We study luminosity- and morphology-dependent clustering in the Southern Sky Redshift Survey 2 (SSRS2, da Costa et al. 1998). This survey is 99% complete with a limiting magnitude of $m_B = 15.5$ within the region $-40^\circ \leq \delta \leq -2.5^\circ$ and $b \leq -40^\circ$ and the region $\delta \leq 0^\circ$ and $b \geq 35^\circ$. We will focus on a volume-limited subsample with $100h^{-1}\text{Mpc}$ depth with 1179 galaxies. We obtained the same results looking at samples with different limiting depths (see Sect. 4.5). In Sect. 4.6 we compare with the results from IRAS selected samples.

4.1. Luminosity as a continuous mark

For a galaxy at a distance $r_i = |\mathbf{x}_i|$ from our galaxy with a magnitude $\text{mag}(\mathbf{x}_i)$ the luminosity L_i is proportional to $r_i^2 10^{-0.4 \text{mag}(\mathbf{x}_i)}$. Since we look at normalized quantities, the absolute scaling of the luminosity is unimportant, and we assign to a galaxy at \mathbf{x}_i the mark $m_i = r_i^2 10^{-0.4 \text{mag}(\mathbf{x}_i)}$. To estimate k_{mm} , var , and cov we show the results obtained with the estimator without boundary corrections, which is distinguished by its simplicity and unbiasedness. The other estimators gave fully consistent results. A systematic examination of the estimators further justifying this approach is given in Appendix A. The errorbars for the case of no luminosity segregation were estimated by randomly redistributing the marks of the galaxies, keeping their positions in space fixed.

Already at a first glance Fig. 2 reveals that all test quantities show evidence of luminosity segregation at a high level of significance, especially k_{mm} and var . The increasing k_{mm} towards small scales supports the hypothesis that bright galaxies exhibit stronger clustering than the dim ones (k_m shows the same feature). The strong signal of var is a result which escaped previous analyses; the luminosity *fluctuations* of galaxies with a neighbor closer than $15h^{-1}\text{Mpc}$ are enhanced, showing that the luminosity distribution is broader for these galaxies in addition to their higher mean luminosity as detected by k_{mm} . Both k_{mm} and var show a signal out to $15h^{-1}\text{Mpc}$, indicating that luminosity segregation is not only confined to clusters of galaxies. The covariance cov measures the correlations between the luminosities on *both* galaxies. It shows only weak evidence for luminosity segregation on large scales, however, on scales smaller than $3h^{-1}\text{Mpc}$, the $\text{cov} > 0$ indicates an excess correlation between the luminosities of two galaxies: Close pairs of galaxies tend to assume similar luminosities. At $r \sim 10h^{-1}\text{Mpc}$, k_{mm} and especially var show a second peak, indicating that the average luminosity of the galaxy pairs and the fluctuations of the luminosity on each galaxy are enhanced. cov shows a negative minimum corresponding to an increased diversity between the luminosities of the two galaxies. Clearly this is at most a two- σ result, however these features also appear in volume-limited samples with different depths.

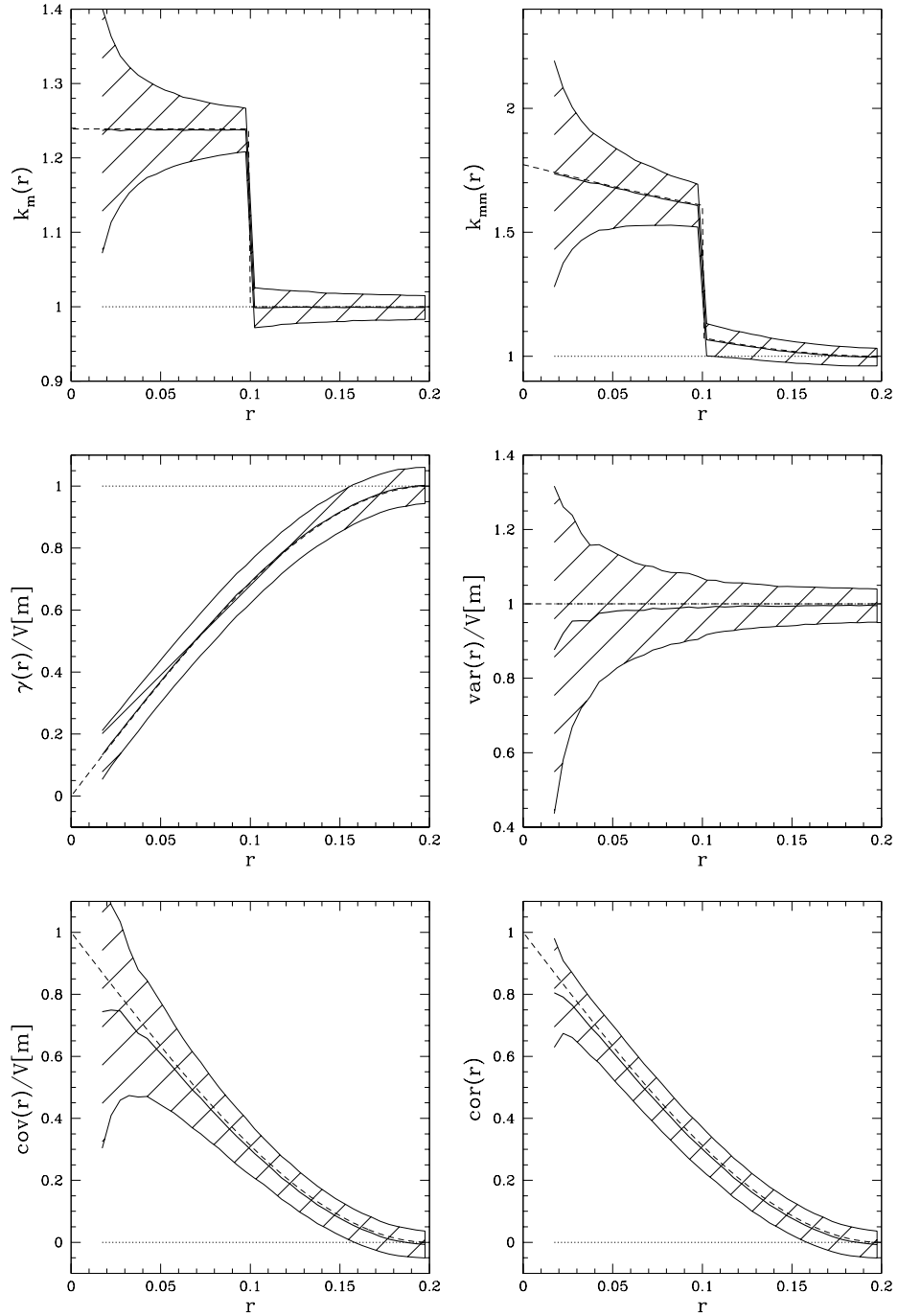


FIG. 1.— The $k_m(r)$, the $k_{mm}(r)$, the normalized $\gamma(r)/V$ and $var(r)/V$, and the covariances $cov(r)$ and $cor(r)$ for a marked Poisson process with number density of 1000 inside the unit box. The points were marked with $N_i(0.1)$. The dashed line is the theoretical result, the shaded area marks the 1σ range estimated from 5000 simulations, and the dotted line is the result for randomly distributed marks. r is given in units of the box-length.

4.2. The random field model

To understand the data in more detail we compare with a particular model for marked point processes which shows mark segregation (Walder & Stoyan 1996). In the *random field model* the marks m_i are assigned to the points \mathbf{x}_i of a (unmarked) point process using an *independent* random field $u(\mathbf{x})$: $m_i = u(\mathbf{x}_i)$. This is a basic model in geo-statistics (see e.g., Cressie 1991). If the point process and the random field are homogeneous, so is the marked point process. In this case one obtains for $r > 0$ (Walder & Stoyan 1996)

$$k_{mm}(r) = \frac{1}{\bar{m}^2} \mathbb{E}[u(0)u(r)], \quad (25)$$

and

$$\gamma(r) = \frac{1}{2} \mathbb{E} [(u(0) - u(r))^2]. \quad (26)$$

Here, \mathbb{E} is the average over several realizations of the random field, thus $\mathbb{E}[u(0)u(r)]$ is the covariance of the field. Using well-known properties of random field covariances (Adler 1981; Walder & Stoyan 1996), a relation for the random field model can be derived:

$$\gamma(r) = \mathbb{E} [u(0)^2] - \bar{m}^2 k_{mm}(r) = V + \bar{m}^2 - \bar{m}^2 k_{mm}(r). \quad (27)$$

This enables us to test whether a marked point process may be understood in terms of the random field model. – Note, that in the random field model the marks are given by an underlying random field, which is not affected by the spatial distribution of the points. This does not cover the general case, where the marks on the points may be influenced by spatial interactions of the points, as in the marked Poisson process in Sect. 3.2. Indeed, the relation (27) is not fulfilled for this model as inferred directly from Fig. 1.

From Fig. 3 we see that for the galaxy distribution the estimated variogram $\gamma(r)$ and the $\gamma^{\text{rf}}(r)$, calculated from Eq. (27), show the opposite behavior. Hence, the luminosity segregation observed in this galaxy sample can not be described by a random field model. Therefore, the luminosity of a galaxy does not trace an independent luminosity field, but rather depends on the spatial interactions with other galaxies. Such an interaction is expected physically in clusters of galaxies, where galaxies merge. Beyond cluster scales this “interaction” may be caused by a common origin in the same large-scale feature of the density distribution.

4.3. Luminosity classes as discrete marks

Now we split the volume-limited sample with $100h^{-1}\text{Mpc}$ depth into three distinct subsamples with 393 galaxies each. These subsamples consist of luminous, medium and dim galaxies, labeled with l , m and d respectively. The conditional cross-correlation functions C_{dd} , C_{dm} , C_{dl} , C_{mm} , C_{ml} , C_{ll} are shown in Fig. 4, estimated from the volume-limited sample with $100h^{-1}\text{Mpc}$ depth using the estimator employing no boundary correction. They show that our above interpretation of $k_{mm}(r)$ based on Fig. 2 points into the right direction. At scales up to $5h^{-1}\text{Mpc}$, the bright galaxies cluster more strongly than the other ones, this effect is at the expense of the dim galaxies, the galaxies with medium luminosities do not contribute to luminosity segregation. However, an analysis based on luminosity classes cannot explain the strong peak of var and cov at small scales since both embody *fluctuations* of the marks. Note, that this partition in luminous, medium and dim galaxies is arbitrary and neither physically justified nor suggested directly by the data. We also divided the sample into two luminosity classes of equal size. Here the cross-correlations are all compatible with the randomized results and no luminosity segregation seems to be present. This emphasizes the discriminative power of the continuous mark correlation functions: The conditional cross-correlation functions for the binned marks may be blind to luminosity segregation. But with a carefully adapted binning they are able to strengthen the conclusions obtained with the continuous mark-correlations functions.

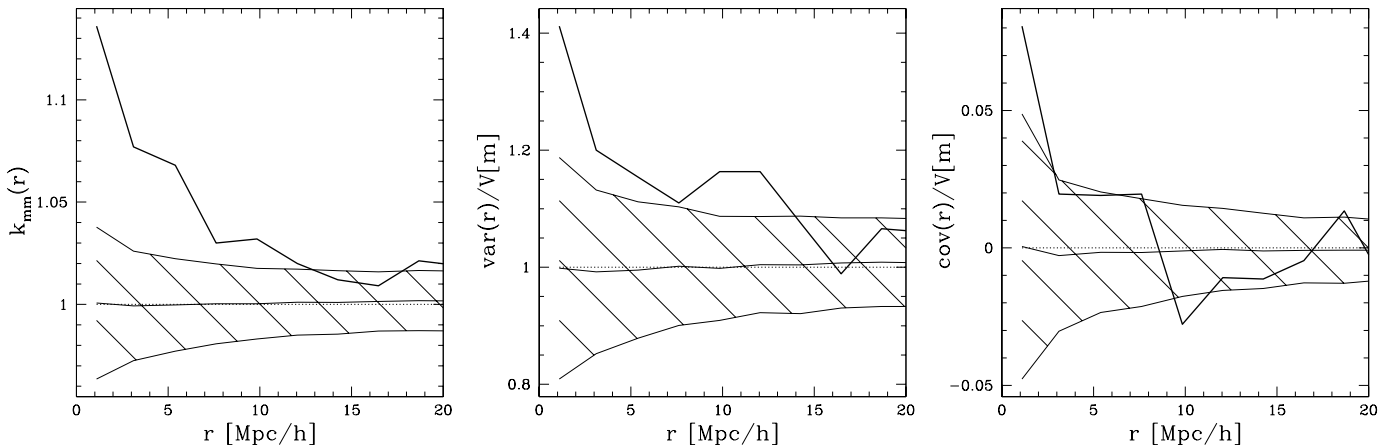


FIG. 2.— The mark-correlation functions for a volume-limited subsample of the SSRS2 with a depth of $100h^{-1}\text{Mpc}$. The shaded areas denote the $1-\sigma$ error for randomized marks estimated from 1000 realizations.

4.4. Morphological types as discrete marks

Using the morphological type of a galaxy as a mark we investigate morphological segregation using the conditional cross-correlation functions defined in Sect. 3.1.2.

The morphological classification of the galaxies in the SSRS2 catalog was compiled from different sources. So, only wide classes will give reliable results (da Costa et al. 1998). We compare the clustering properties of two classes, consisting of spiral, irregular and peculiar galaxies, labeled with l (late type), and elliptical and lenticular galaxies, labeled with e (early type). We discard the small fraction of unclassified galaxies. In Fig. 5 the conditional cross-correlation functions $C_{ee}(r)$, $C_{el}(r)$, $C_{ll}(r)$ are shown, estimated from the volume-limited sample with $100h^{-1}\text{Mpc}$ depth, using no boundary correction.

The results demonstrate, that the clustering properties of the SSRS2-galaxies depend on morphology. Although the late-type galaxies predominate the catalog, especially the small-scale clustering is disproportionately due to pairs of early-type galaxies. In Subsect. 4.3 we saw that the luminous galaxies tend to cluster stronger. At this point, the question arises, whether the morphology segregation is a possible explanation of the luminosity segregation or vice versa. We will discuss the connection between both sorts of mark segregation in Sect. 6.1.

4.5. Error estimates

In the preceding sections we have shown results for a volume-limited sample with $100h^{-1}\text{Mpc}$ depth. We also considered volume-limited samples with a limiting depth of $60h^{-1}\text{Mpc}$, $80h^{-1}\text{Mpc}$ and $120h^{-1}\text{Mpc}$, all giving similar results. Moreover, the results do not change if we use luminosity distances instead of Euclidean and apply a type-dependent K -correction as used by Benoist et al. (1996) (see Fig. 6).

Systematic errors may occur, since we performed our analysis in redshift space, i.e., we estimate the luminosity L of a galaxy using its redshift z : $L \propto z^2 10^{-0.4\text{mag}}$. Therefore peculiar velocities not only change the spatial correlations, but also the values of the marks may be biased in a systematic way. It is difficult to correct for such an effect, since in-fall and streaming motions lead to correlated peculiar velocities. To estimate the order of magnitude of this error we randomly add a line-of-sight peculiar velocity to each galaxy following a Gaussian distribution with zero mean and a width of 300km/s in agreement with the value for the pairwise velocity dispersion in the SSRS2 given by Marzke et al. (1995). In randomizing the radial velocities independently we overestimate this error since correlated pairs are eventually torn apart⁶. Repeating this procedure several times we can show that the mean values of k_{mm} , var and cov do not change compared to the results in Fig. 2. The additional fluctuations introduced by this procedure are smaller than the statistical errors quantified by randomizing the marks, as can be seen in Fig. 6. Both k_{mm} and var show a signal outside the one- σ range of this luminosity error combined with the statistical errors, whereas cov is becoming marginally consistent.

Note, that in volume-limited samples a special sort of Malmquist-bias may influence the luminosities: The luminosities are estimated using the flux and the redshift as the distance indicator. Hence the distance is influenced by the individual peculiar velocity of the galaxy. Consider a shell at distance r . For geometrical reasons more galaxies from the outer side get scattered into the shell than galaxies get scattered outside. Hence, in the mean more galaxies are assigned too small distances resulting in underestimated luminosities. Considering only galaxies with a distance smaller than $90h^{-1}\text{Mpc}$ in the volume-limited sample with $100h^{-1}\text{Mpc}$ depth we obtain nearly identical results for the mark-correlation functions. Therefore, this sort of bias does not affect our analysis.

4.6. IRAS selected galaxies

⁶In adding random peculiar velocities we also account for possible errors within the measurements of the redshifts, which are in fact much smaller than the imprints of peculiar velocities.

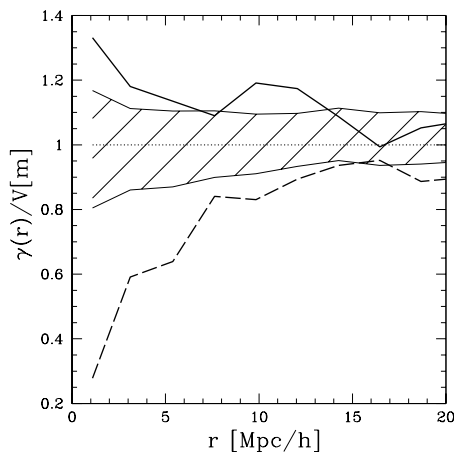


FIG. 3.— Both the normalized variogram $\gamma(r)/V$ (solid line) and the normalized $\gamma^{rf}(r)/V$ (dashed line), calculated according to Eq. (27) are shown. The shaded area is marking the 1- σ region for $\gamma(r)/V$ with randomized marks.

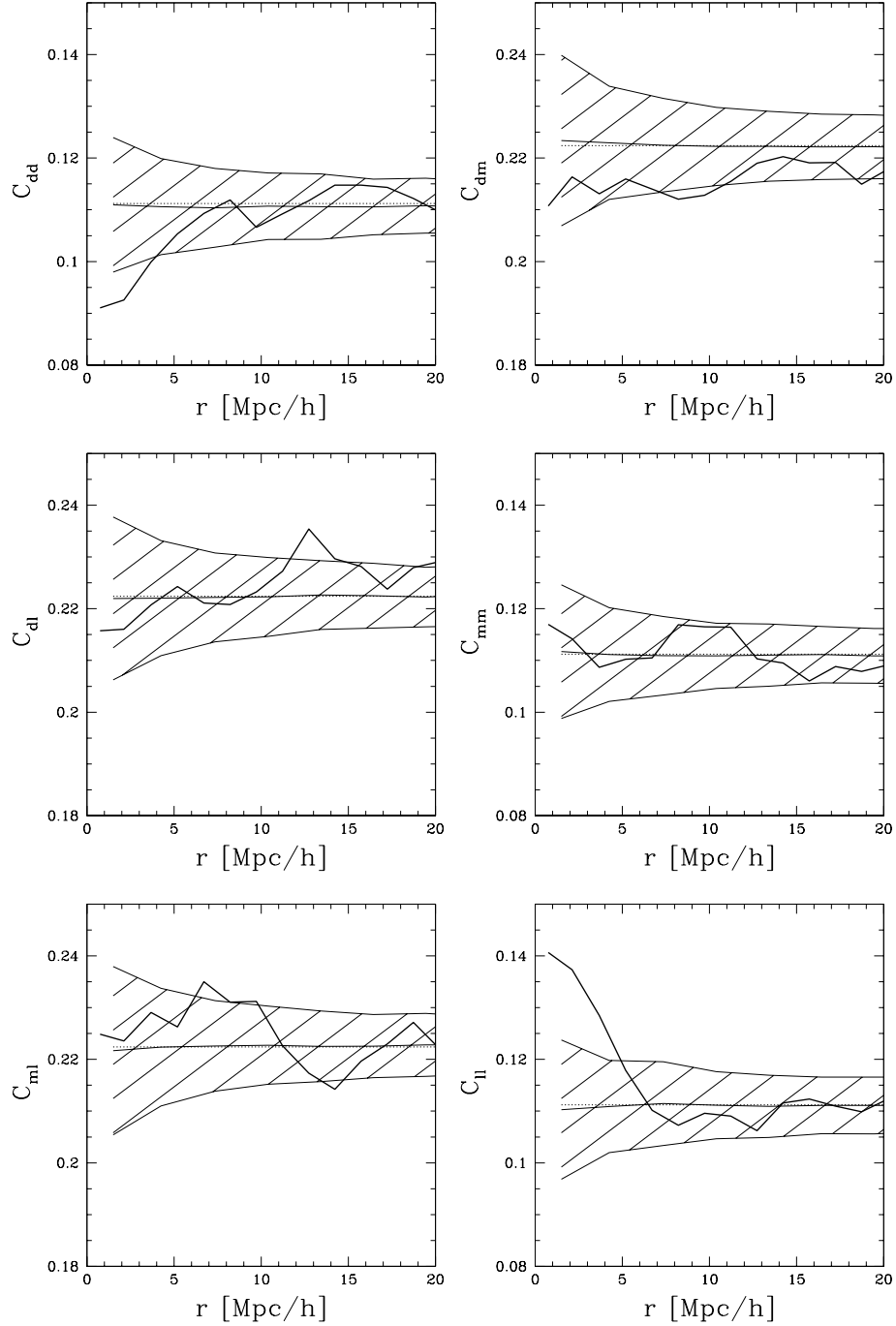


FIG. 4.— The conditional cross-correlation functions of dim (d), medium (m), and luminous (l) galaxies in the volume-limited sample with $100h^{-1}\text{Mpc}$ depth. The shaded $1-\sigma$ region was determined from 1000 realizations with randomized marks.

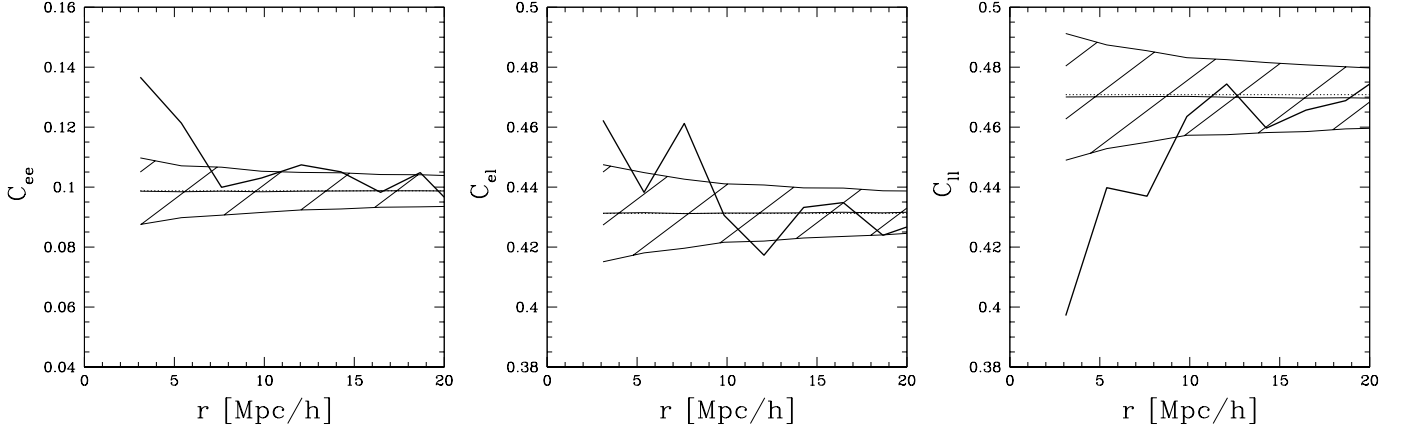


FIG. 5.— The conditional cross-correlation functions of early (*e*) and late (*l*) type galaxies in the volume-limited sample with $100h^{-1}\text{Mpc}$ depth. The $1\text{-}\sigma$ region was determined from 1000 realizations with randomized marks.

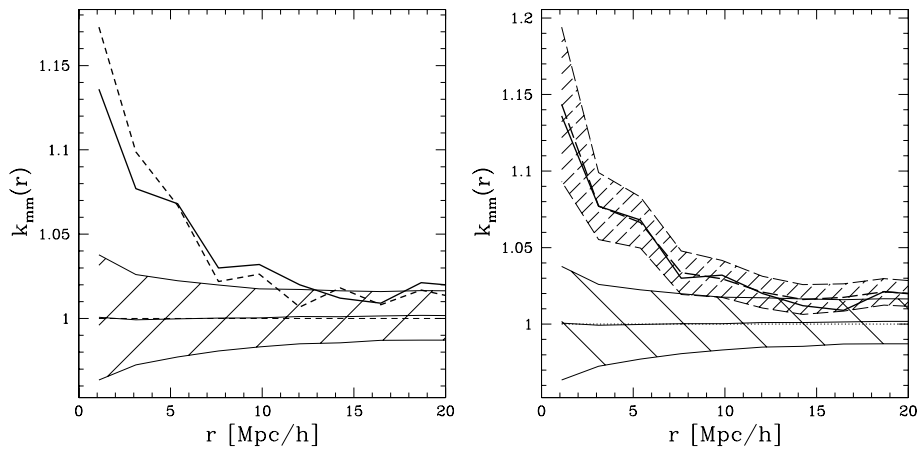


FIG. 6.— In the left figure the $k_{mm}(r)$ function is shown calculated from the measured magnitudes using the Euclidean distances (solid line) compared to the $k_{mm}(r)$ function calculated from K -corrected magnitudes using the luminosity distances. In the right plot again the “pure” $k_{mm}(r)$ function (solid line) is compared to the $k_{mm}(r)$ function calculated with randomized peculiar velocities (shaded area with dashed lines). The shaded area with solid lines corresponds to the results with randomized marks.

Up to now we investigated luminosity segregation in the optically selected SSRS2 catalog, with the luminosities estimated from the B-magnitude. To see how our results depend on the selection criteria imposed on the catalog we look at the mark correlations determined from the infrared selected IRAS 1.2 Jy and PSCz galaxy catalogs (for details see Fisher et al. 1995, Saunders et al. 2000).

We analyze 2259 galaxies in the volume-limited sample of the PSCz galaxy catalog with a depth of $100h^{-1}\text{Mpc}$ inside the mask given by Saunders et al. (2000). Similarly to Sect. 4 we use $m_i = r_i^2 f(\mathbf{x}_i)$ as a continuous mark, proportional to the luminosity of the galaxy at a distance of $r_i = |\mathbf{x}_i|$ with an observed flux $f(\mathbf{x}_i)$ at 60 microns. From Fig. 7 we conclude that no significant luminosity segregation is present in the PSCz galaxy catalog. The same result holds for volume-limited samples with different depths, and for volume-limited samples extracted from the IRAS 1.2 Jy catalog. This confirms the results by Bouchet et al. (1993) from the IRAS 1.2 Jy and especially the investigation of the PSCz by Szapudi et al. (1999) who used a variant of the conditional cross-correlations discussed in Subsect. 3.1.2. Similarly, only a weak dependence on spectral features was reported by Mann et al. (1996) for the QDOT catalog. In Sects. 6.2 and 6.3 we will see that the luminous early-type galaxies play a dominant role for luminosity and morphology segregation. This is supported by the negative results from these IRAS selected samples, since early-type galaxies are significantly underrepresented in infrared-selected galaxy samples.

There is however an interesting feature in the deeper volume-limited samples from the PSCz. Both $k_{mm}(r)$ and $\text{var}(r)$ are consistent with a random mark distribution, but the covariance $\text{cov}(r)$ shows an almost three- σ peak near $r = 20h^{-1}\text{Mpc}$. This increased covariance at $20h^{-1}\text{Mpc}$ is currently beyond an explanation, however the feature is also visible in volume-limited samples with $200h^{-1}\text{Mpc}$ and $300h^{-1}\text{Mpc}$ depth, and stable against distance cuts and different binning.

5. LUMINOSITY SEGREGATION VIA AMPLITUDES

Previous investigations detecting luminosity segregation have used a sequence of volume-limited samples and compared the correlation amplitude of the two-point correlation function $\xi(r)$ (see e.g., Willmer et al. 1998). In Subsect. 5.1 we show how this can be incorporated into the more general formalism provided in Sect. 2. In Subsect. 5.2 we reassess the arguments given by Coleman & Pietronero (1992) showing that there is a degeneracy between a scale-invariant point distribution and luminosity segregation *if* the analysis is based on the amplitudes of ξ . The mark characteristics introduced in Subsect. 3.1 do not suffer from this artifact as shown in Subsect. 5.3. This strengthens our conclusions in Sect. 4 that there is indeed luminosity and morphological segregation.

5.1. Luminosity segregation from a series of volume-limited samples

Consider a flux-limited sample with limiting flux f_{lim} . Every galaxy at a distance $|\mathbf{x}_i|$ with observed flux $L_i/(4\pi|\mathbf{x}_i|^2)$ larger than some limiting flux f_{lim} is included in the sample. We construct volume-limited subsamples by introducing a limiting depth R and a limiting luminosity L_{lim} with $L_{\text{lim}}/(4\pi R^2) = f_{\text{lim}}$ and by admitting only galaxies with $|\mathbf{x}| < R$ and $L > L_{\text{lim}}$. In such a volume-limited sample⁷ the observed number density $\rho_{1,R}^S(\mathbf{x}) = \rho_{1,R}^M$ is spatially constant

$$\rho_{1,R}^S = \rho \int_{L_{\text{lim}}}^{\infty} dL \rho_1^M(L), \quad (28)$$

if the underlying galaxy pattern is homogeneous.

⁷In general, we have more freedom in constructing volume-limited samples: varying R and L_{lim} independently, as long as the constraint: $R^2 < \frac{L_{\text{lim}}}{4\pi f_{\text{lim}}}$ is respected. Holding L_{lim} fixed, we can vary R and look, whether the statistical properties, e.g., the amplitude of the correlation function ξ , differs between these samples. This would allow to test for fractal spatial structures independent from luminosity segregation.

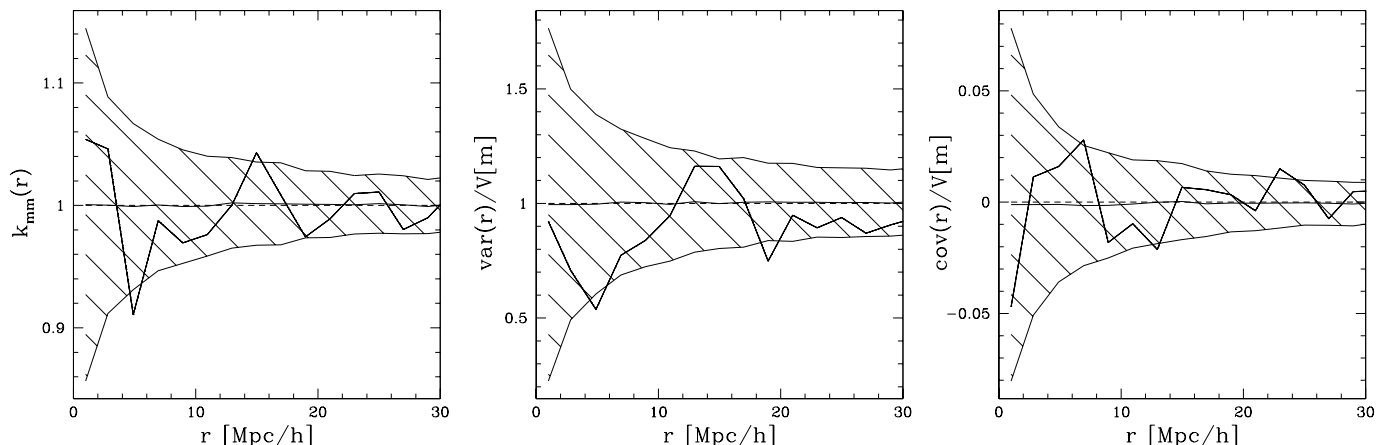


FIG. 7.— The mark-correlation functions for a volume-limited subsample of the PSCz catalog with a depth of $100h^{-1}\text{Mpc}$. The shaded areas denote the $1\text{-}\sigma$ error for randomized marks estimated from 1000 realizations.

For two–point properties we can proceed similarly. The spatial two–point density in the volume–limited samples for $|\mathbf{x}_1| < R$ and $|\mathbf{x}_2| < R$ is

$$\rho_{2,R}^S(\mathbf{x}_1, \mathbf{x}_2) = \int_{L_{\text{lim}}}^{\infty} dL_1 \int_{L_{\text{lim}}}^{\infty} dL_2 \rho_2^{SM}((\mathbf{x}_1, L_1), (\mathbf{x}_2, L_2)). \quad (29)$$

Using the definition (11) of the conditional probability density \mathcal{S}_2 and the assumption (7) we get

$$\rho_{2,R}^S(\mathbf{x}_1, \mathbf{x}_2) = \mathcal{N}_2 \int_{L_{\text{lim}}}^{\infty} dL_1 \int_{L_{\text{lim}}}^{\infty} dL_2 \mathcal{S}_2(\mathbf{x}_1, \mathbf{x}_2 | L_1, L_2) \rho_1^M(L_1) \rho_1^M(L_2). \quad (30)$$

With $r = |\mathbf{x}_1 - \mathbf{x}_2|$, the two–point correlation function $\xi_R(r)$ in a volume–limited sample is then

$$\xi_R(r) + 1 = \frac{\mathcal{N}_2}{\left(\rho \int_{L_{\text{lim}}}^{\infty} dL \rho_1^M(L)\right)^2} \int_{L_{\text{lim}}}^{\infty} dL_1 \int_{L_{\text{lim}}}^{\infty} dL_2 \mathcal{S}_2(\mathbf{x}_1, \mathbf{x}_2 | L_1, L_2) \rho_1^M(L_1) \rho_1^M(L_2). \quad (31)$$

If no luminosity segregation is present, $\mathcal{S}_2(\mathbf{x}_1, \mathbf{x}_2 | L_1, L_2) = \rho_2^S(\mathbf{x}_1, \mathbf{x}_2) / \mathcal{N}_2$ and therefore:

$$\xi_R(r) = \xi(r). \quad (32)$$

If, on the other hand, the clustering of the galaxies does depend on the luminosities, the two–point correlation function is different between volume–limited samples of varying depths, and also differs from the two–point correlation function of all galaxies.

As an illustration we calculate $\xi_R(r)$ from volume–limited samples of the SSRS2 with increasing limiting depth R . Our results in Fig. 8 completely agree with the results reported by Willmer et al. (1998), showing a higher amplitude of $\xi_R(r)$ for the deeper volume–limited samples. See also the comprehensive investigations of Cappi et al. (1998) and Benoist et al. (1999). We used several estimators for the two–point correlation function (Kerscher 1999), including the minus estimator shown in Fig. 8 and found that this behavior of the amplitude is independent of the estimator.

5.2. Faking luminosity segregation

In this section we illustrate the argument by Coleman & Pietronero (1992) who showed that there is a degeneracy between luminosity segregation determined with the standard method (Subsect. 5.1) and a fractal galaxy distribution. Indeed, a general inhomogeneous galaxy distribution can fake a sort of “luminosity segregation”. Here, we use a “fractal point set” as a simple, yet analytically tractable model for general inhomogeneous point distributions.

The argument is based on the scaling behavior of the number of points inside a sample $N(R) \propto R^D$ for a fractal point set in a sample with linear extent R , where D is the (correlation–) dimension. For a fractal point set the two–point correlation function behaves like

$$\xi_R(r) + 1 \propto R^D r^{D-3}, \quad (33)$$

with an amplitude of ξ_R depending on the extent of the sample (for details see Sylos Labini et al. 1998). We illustrate this in Fig. 8 showing that fractal correlations according to formula (33) can mimic a behavior of ξ_R as observed in the galaxy data.

To summarize, the behavior of ξ in a series of volume–limited samples can be explained either by a fractal point distribution or luminosity segregation or both. So ξ does not seem to be a good method to assess one of both claims. Note, that Pietronero’s argument is based on the assumption that no luminosity segregation is present.

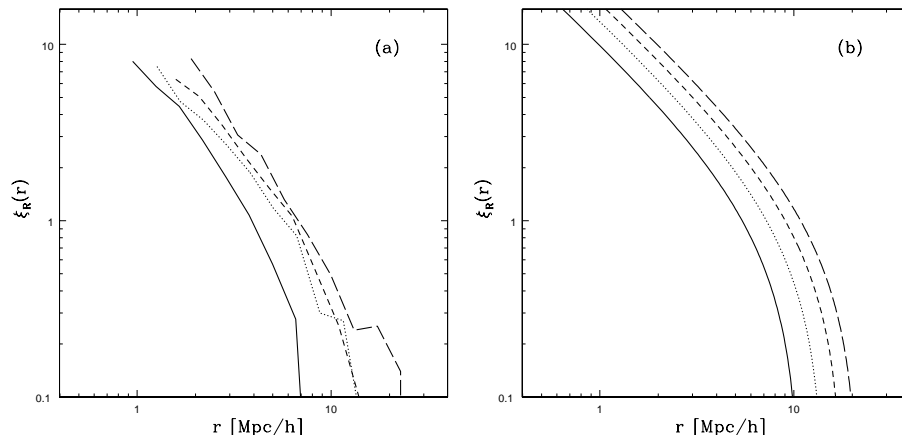


FIG. 8.— In plot (a) the two–point correlation functions $\xi_R(r)$ for volume–limited samples of the SSRS2 with $R = 60h^{-1}\text{Mpc}$ (solid), $80h^{-1}\text{Mpc}$ (dotted), $100h^{-1}\text{Mpc}$ (short dashed) and $120h^{-1}\text{Mpc}$ (long dashed) depth are shown. In plot (b) the two–point correlation functions $\xi_R(r)$ for a fractal with fractal dimension $D = 2$ are shown, with the same increasing depths R mimicking luminosity segregation.

5.3. Robustness of mark–correlation functions

In the preceding section we have seen that to search for luminosity segregation employing the amplitude of ξ_R may be uncertain. Now we show that the mark characteristics introduced in Subsect. 3.1 do not suffer from this degeneracy.

All the quantities we used to investigate luminosity and morphological segregation were defined using the average $\langle f \rangle_P(r)$ over a weight function f . With $\langle f \rangle_P(r)$ we look at the averages of some mark–dependent weight function $f(m_1, m_2)$, under the condition that the points holding the marks are separated by r . We do not investigate the spatial distribution of the points. As can be seen directly from Eq. (13) the spatial two–point correlations are “divided out”. Hence, quantities like $\langle f \rangle_P(r)$ are not only well–defined for homogeneous point distributions, but also give reliable results for inhomogeneous point distributions like fractals.

To illustrate this we use a “fractal point set” kindly provided by Alessandro Amici. This fractal is a three–dimensional realization of the random– β model with a fractal dimension of two. On a randomly selected set of points from this fractal we distribute marks chosen randomly out of $[0, 1]$. This resembles a volume–limited sample with no luminosity segregation. We estimate the mark–correlation functions using the estimator without boundary corrections. The function $k_{mm}(r)$ shown in Fig. 9 gives the correct result that no mark correlation is present. Hence, our methods give stable results even on such an inhomogeneous point distribution. This is also the case for all other functions and for any estimator considered (Appendix A). Therefore, our results obtained from the SSRS2 galaxy survey discussed in Sect. 4 can not be explained with a scale–invariant spatial distribution, showing no luminosity, alone.

There is also a more technical advantage of our method: to estimate the correlation function $\xi(r)$ one has to employ boundary corrections. Quantities like k_{mm} only use conditional probabilities and may be estimated without boundary corrections (see Appendix A), reducing the estimators’ variance.

6. THE MORPHOLOGY–DENSITY RELATION

The morphology–density relation states that inside clusters, in regions with a high (surface) density of galaxies, the abundance of early–type galaxies is enhanced whereas the abundance of late–type galaxies is reduced (Dressler 1980). This relation is very well established, and therefore it seems natural to ask whether the observed luminosity segregation can be explained by the morphology–density relation alone. In this section we present a number of reasons why this is *not* the case.

As a first test we discarded all galaxies in a spherical region with $1.5h^{-1}\text{Mpc}$ and also $3h^{-1}\text{Mpc}$ radius around the APM clusters (Dalton et al. 1997), and conduct a analysis similar to the one in Subsect. 4.1 restricted to the intersection of the SSRS2 and the APM cluster catalog. The mark correlation functions did not show any significant change. This may not be decisive, since only a few of the (rich) APM clusters are included; however, it supports our view that the observed luminosity segregation is not caused by clusters of galaxies alone.

But in the spirit of the morphology–density relation, one could try to explain the observed luminosity segregation in the following way: the two populations of galaxies, the early– and the late–type galaxies, cluster in a different way (which is, e.g., manifest in the morphology–density relationship and in the observed morphology segregation Sect. 4.4). If these classes show different average luminosities, the morphology–density relation will generate the luminosity segregation. This is the main idea behind the two–species model discussed below. A first indication, that this kind of model is not able to explain luminosity segregation, comes from the observation, that both early– and the late–type galaxies show very similar luminosity distributions within the volume–limited sample we considered.

We conduct additional tests of this idea, which allow for a further understanding of the luminosity segregation: we consider the two–species model in Subsect. 6.1 in more detail, and we investigate the early– and late–type galaxies separately in Subsect. 6.2; moreover, we look for morphology segregation in dim and luminous subsamples separately in Subsect. 6.3.

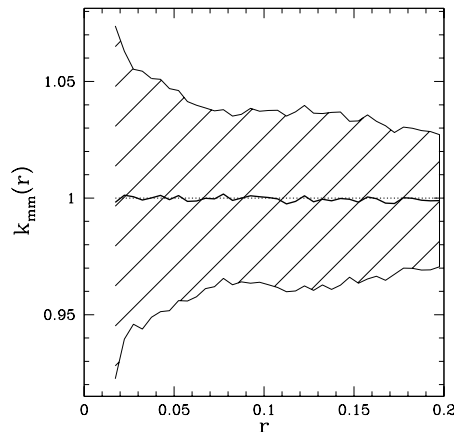


FIG. 9.— The $k_{mm}(r)$ for a fractal point distribution with random marks and number density 1000 inside the unit box. The shaded area marks the $1\text{-}\sigma$ range estimated from 1000 simulations, and the dotted line is the theoretical expectation. r is given in units of the box–length.

6.1. *The two-species model*

As already outlined above, in the two-species model we consider two subpopulations of galaxies, with different spatial clustering and a different mark distribution. Within each class there is no mark segregation. Thus this model explains in a very simple way how mark correlations arise from the spatial interplay of the two classes of galaxies. The subclasses will be formed by early- (e) and late-type (l) galaxies.

Let ρ_l , \bar{m}_l , V_l denote the number density, the mean mark, and the variance of the marks of galaxies of type l , respectively, and similarly for subclass e . The one-point mark distributions are denoted by $\rho_{1,e}^M(m)$ and $\rho_{1,l}^M(m)$. The spatial (cross-) correlations are given by $\xi_{ee}(r)$, $\xi_{ll}(r)$, and $\xi_{el}(r)$ (symmetrically defined in e and l , i.e., $(\xi_{el} + \xi_{le})/2$). We use the morphological type and the luminosity as components of a compound mark $\mathbf{m} = \{t, m\}$, where $t \in \{e, l\}$ denotes the morphological type and m is the luminosity of the galaxy. The two-point properties within the two-species model are then given by:

$$\begin{aligned} \rho_2^{SM}((\mathbf{x}_1, \{t_1, m_1\}), (\mathbf{x}_2, \{t_2, m_2\})) = \\ \delta_{t_1 e} \delta_{t_2 e} \rho_e^2 \rho_{1,e}^M(m_1) \rho_{1,e}^M(m_2) (1 + \xi_{ee}(r)) + \delta_{t_1 l} \delta_{t_2 l} \rho_l^2 \rho_{1,l}^M(m_1) \rho_{1,l}^M(m_2) (1 + \xi_{ll}(r)) \\ + (\delta_{t_1 e} \delta_{t_2 l} \rho_{1,e}^M(m_1) \rho_{1,l}^M(m_2) + \delta_{t_1 l} \delta_{t_2 e} \rho_{1,l}^M(m_1) \rho_{1,e}^M(m_2)) \rho_e \rho_l (1 + \xi_{el}(r)). \end{aligned} \quad (34)$$

With $q_l = \rho_l / (\rho_l + \rho_e)$, $q_e = 1 - q_l$, the combined two-point correlation is function

$$1 + \xi(r) = q_e^2 (1 + \xi_{ee}(r)) + q_l^2 (1 + \xi_{ll}(r)) + 2q_e q_l (1 + \xi_{el}(r)), \quad (35)$$

and using the definitions in Sect. 3.1.1 one may calculate the luminosity correlation functions for this specific model. We measured q_e , ξ_{ee} , as well as \bar{m}_e , V_e etc. in the volume-limited sample with $100h^{-1}$ Mpc depth from the SSRS2. Using these quantities we calculated the mark-correlation functions for the two-species model. In Fig. 10 we compare the *var* function from the two-species model with the actual observed values (similar results are obtained for k_{mm} and *cov*). Obviously, the two-species model is not able to explain the observed luminosity-correlations. This shows that the spatial interplay between different morphological types, as suggested by the morphology-density relation, is only in part responsible for the observed luminosity segregation. A necessary ingredient is that luminosity segregation is already present in one of the subclasses at least (see the next section).

The results for the two-species model shown in Fig. 10 were obtained selfconsistently from the empirically determined parameters as given by the division of the sample into early- and late-type galaxies. We may go further and treat the two-species model as a toy model with scale-invariant (cross-) correlation functions (e.g., $\xi_{ee} \propto r^{-\gamma}$) and free parameters \bar{m}_e etc. to fit the data. However, we find that an acceptable qualitative description of the observed luminosity segregation in terms of this model is only satisfied when the parameters of the two-species model are highly unrealistic.

6.2. *Early- and late-type galaxies separately*

As a second test, we split the $100h^{-1}$ Mpc volume-limited sample from the SSRS2 into two subsamples consisting out of early- and late-type galaxies each. Using the luminosity as the (continuous) mark, we look for luminosity segregation similarly to the investigations in Sect. 4.1. From Fig. 11 it is evident that both subpopulations show luminosity segregation, but the main contribution comes from early-type galaxies. The late-type galaxies show a small signal in k_{mm} only. Clearly, with this kind of analysis we do not pick up features intrinsic to the interplay between early- and late-type galaxies, which may add a further contribution to the observed luminosity segregation (Fig. 2).

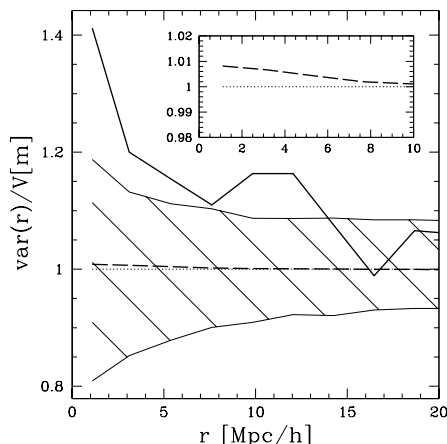


FIG. 10.— The mark-correlation function $var(r)$ for a volume-limited subsample of the SSRS2 with a depth of $100h^{-1}$ Mpc (solid line) compared with the mark-correlation function calculated from the two-species model (dashed line). The shaded area denotes the $1-\sigma$ error for randomized marks estimated from 1000 realizations. The inset compares the case of no luminosity segregation (dotted line) and the prediction of the two-species model (dashed line)

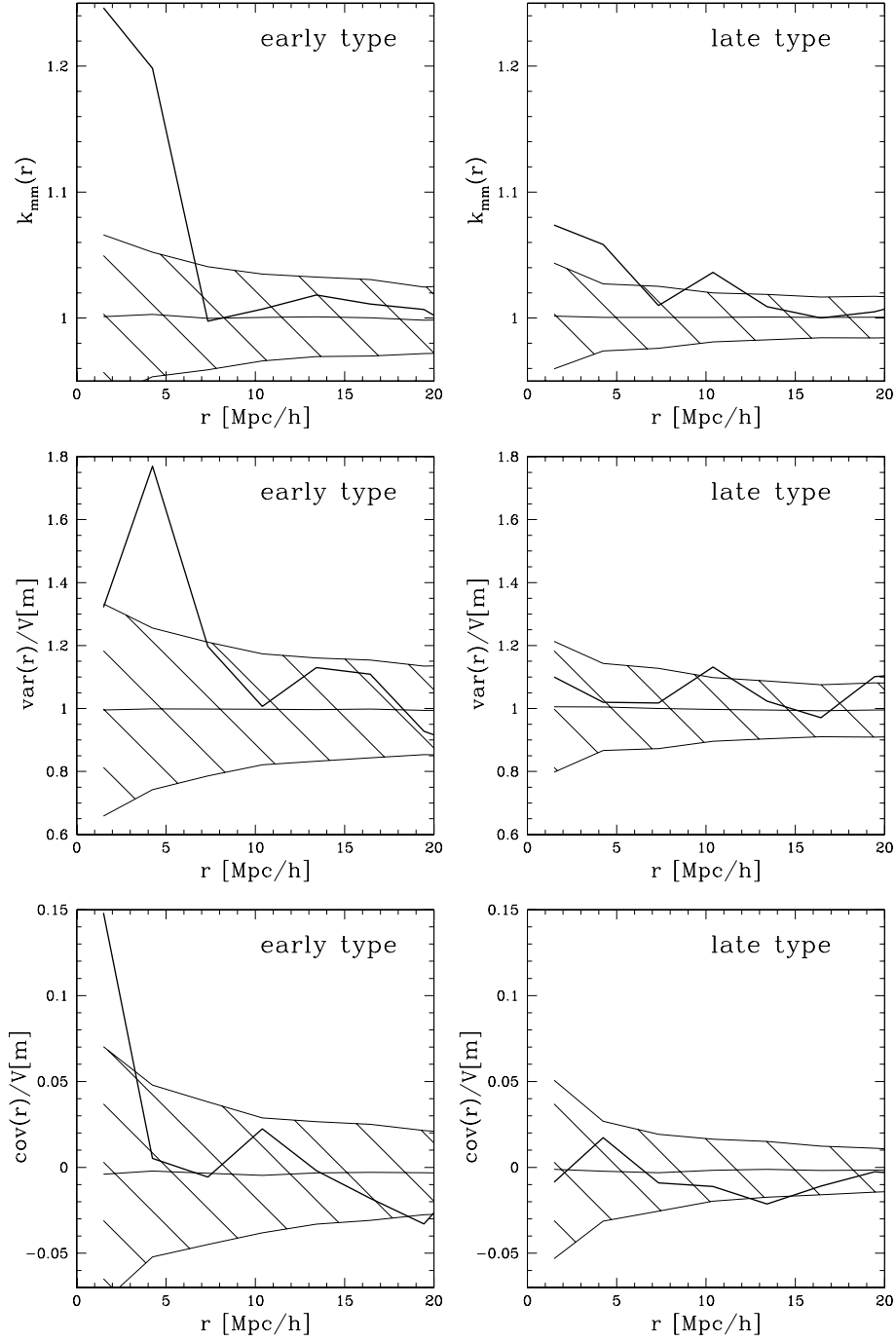


FIG. 11.— The mark–correlation functions for a the early–type and late–type galaxies from the volume–limited sample of the SSRS2 with a depth of $100h^{-1}\text{Mpc}$. The shaded areas denote the $1-\sigma$ errors for randomized marks estimated from 1000 realizations.

6.3. *The other way round?*

So far, our results show clearly, that the luminosity segregation is not a pure effect of the morphology segregation. To investigate the opposite case, where the morphology segregation is caused by the luminosity segregation, we split the volume-limited sample with $100h^{-1}\text{Mpc}$ depth into two equally sized luminosity classes, with *dim* and *luminous* galaxies, respectively. For each of these samples we calculate the conditional cross-correlations between early- and late-type galaxies. The strong (conditional) correlations $C_{ee}(r)$ of early-type galaxies on small scales are now only visible in the sample of *luminous* galaxies, confirming the trends reported by Willmer et al. (1998). The conditional anticorrelation indicated by the $C_{ll}(r)$ of the late type galaxies on small scales is present in both subsamples but more pronounced in the sample of *luminous* galaxies (only $C_{ee}(r)$ is shown in Fig. 12). This test does not allow very strong conclusions, since it is based on an ad-hoc division of the whole sample. A finer division is not feasible, since very few early-type galaxies will populate the subsamples. However, our results strengthen the interpretation that both sorts of mark correlations are irreducible. Neither is the luminosity segregation the source of morphological segregation nor is it the other way around. In particular, the luminous early-type galaxies cluster more strongly than all other galaxies.

7. SUMMARY AND OUTLOOK

The investigation of luminosity and morphology segregation of galaxies has been a scientific task for many years. Our results allow for a new perspective and suggest that both the *methodology* and the *physical interest* should shift slightly.

Methodologically, we discussed luminosity and morphological segregation in the framework of marked point processes. This perspective provides us with a unifying view on morphology and luminosity segregation. Moreover, the mathematical theory of marked point processes provides us with test quantities and models to be compared with the data. In this line we discussed the mark-weighted conditional correlation functions. These functions are not only easy to estimate, but also offer a clear interpretation. They may be applied to a single volume limited sample, a sequence of volume limited samples is not necessary. As a consequence, they break the degeneracy between a fractal spatial structure and luminosity segregation. We suggest that the k_{mm} , var , and cov functions are of special interest for a first test on luminosity segregation. Since several bias-models assume scale-dependent bias, we need quantities like k_{mm} , var , and cov which can unfold the scales at which mass or luminosity segregation is relevant. This is not possible by looking at the amplitude of the two-point correlation function $\xi_R(r)$ alone. Moreover our method allows for a “built in” significance test, by randomly re-shuffling the marks. The conditional cross-correlation functions seem to be useful if mark segregation has already been shown to be present and is to be understood more closely. However, they are based on a division of the whole sample into subpopulations, a division that has to be done carefully. The conditional mark-correlation functions are rather flexible. With the peculiar velocities or the orientations of galaxies treated as marks, the conditional mark correlation functions will allow for a fresh look at the pairwise velocity dispersion and on alignment effects. Our methods can be easily extended to higher-order correlations. In a forthcoming work we will study the mark correlations using higher-order statistics as the J -functions (van Lieshout & Baddeley 1996, Kerscher 1998).

Concerning the physical results, we were not only able to assess luminosity segregation as well as morphological segregation. Rather, our perspective allowed us to ask the question: What is the luminosity and morphological segregation like? Our main results obtained from the SSRS2 survey are:

- The average luminosity of pairs of galaxies and the fluctuations in the luminosity on each galaxy is enhanced for pairs closer than $15h^{-1}\text{Mpc}$. Hence, luminosity correlations are scale-dependent, and they are significant even outside clusters of galaxies. On scales larger than $15h^{-1}\text{Mpc}$ our results indicate that neither luminosity nor morphological segregation is present.

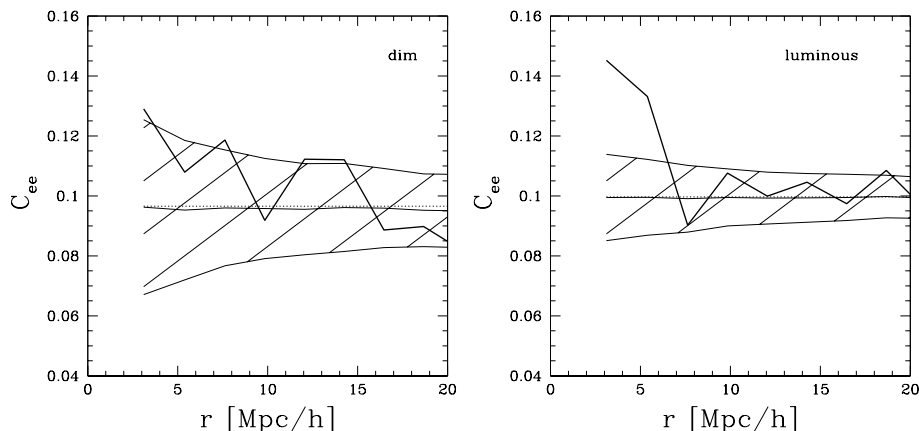


FIG. 12.— The conditional cross-correlation function $C_{ee}(r)$ of early-type galaxies in the luminous and dim subsamples. The $1-\sigma$ region was determined from 1000 realizations with randomized marks.

- The luminosities of galaxies in pairs closer than $3h^{-1}\text{Mpc}$ show an increased covariance – close galaxies preferably have similar luminosities.
- The luminosity segregation is not compatible with the random field model. Thus, the luminosity does not trace an underlying *independent* random field. The luminosity of a galaxy depends on the local clustering and on interactions with other galaxies.
- There is an interesting feature, a small peak, in k_{mm} , var and cov for galaxy pairs with a separation of approximately $10h^{-1}\text{Mpc}$, which is currently beyond an explanation.
- We observe morphological segregation between early- and late- type galaxies for scales smaller than $10h^{-1}\text{Mpc}$. This effect is mainly due to highly luminous galaxies. Especially the luminous early-type galaxies seem to play an important role, both for luminosity and morphology segregation.
- The importance of early-type galaxies for luminosity segregation is confirmed by our analysis of the IRAS samples. These infrared samples exhibit a deficit in early-type galaxies and consequently show no luminosity segregation.
- An inhomogeneous, scale-invariant galaxy distribution, but without luminosity segregation, can not account for the signal seen in k_{mm} , var , and cov . The lowered correlation of the dim galaxies, and the enhanced correlation of the luminous galaxies we found, explains at least in part why the amplitude of the correlation function rises if deeper, i.e., more luminous, galaxy samples are considered.
- With several independent tests we could show that it is not possible to explain the observed luminosity segregation from the morphology–density relation alone.

Nevertheless, a couple of question remain open.

Concerning the data, it seems important to confirm our results using other galaxy surveys. Also the influence of redshift space distortions and of galaxy clusters should be investigated beyond the simple error–estimates presented in Subsect. 4.5 and Sect. 6.

Our methods are directly applicable to volume-limited samples, similar to the usual way of assessing luminosity segregation, where one needs a series of volume-limited samples. Using models for the conditional mark density \mathcal{M}_2 or the mark–correlation functions one may determine the parameters of such models from magnitude-limited surveys directly. Similarly, the influence of mark segregation on the two- and N -point correlations estimated from magnitude-limited surveys can be estimated.

Closely related is the question how strongly the deprojected two- and N -point correlation functions, determined from 2-dimensional galaxy catalogs, are influenced by luminosity segregation. With models for the mark–correlations a refined Limber’s equation may be constructed (see e.g., Gardini et al. 1999). Both, the concerns about magnitude-limited surveys and deprojection formulas will be addressed in future work.

In this article we focused on clarifying the mathematical framework, on the data-analysis, and on the interpretation of the observed luminosity and morphological segregation. The relation to the peak-formalism (Bardeen et al. 1986) and other biasing schemes will be investigated in future work. Understanding the luminosity distribution on the galaxies from dynamical models is the major goal.

We thank Thomas Buchert, Niv Drory, Ulrich Hopp, Roberto Saglia, Dietrich Stoyan, Alex Szalay, Istvan Szapudi and Herbert Wagner for valuable discussions and Alessandro Amici for kindly providing the fractal point set used in Subsect. 5.3. CB and MK acknowledge support from the *Sonderforschungsbereich 375 für Astroteilchenphysik der DFG*. MK acknowledges support from the NSF grant AST 9802980.

REFERENCES

- Adler, R. J. 1981, *The geometry of random fields* (Chichester: John Wiley & Sons)
- Alimi, J.-M., Valls-Gabaud, D., & Blanchard, A. 1988, *A&A*, 206, L11
- Andreon, S., Davoust, E., & Heim, T. 1997, *A&A*, 323, 337
- Bardeen, J. M., Bond, J. R., Kaiser, N., & Szalay, A. S. 1986, *ApJ*, 304, 15
- Benoist, C., Cappi, A., Da Costa, L., Maurogordato, S., Bouchet, F., & Schaeffer, R. 1999, *ApJ*, 514, 563
- Benoist, C., Maurogordato, S., Da Costa, L., Cappi, A., & Schaeffer, R. 1996, *ApJ*, 472, 452
- Binggeli, B., Tarnghi, M., & Sandage, A. 1990, *A&A*, 1228, 42
- Börner, G., Mo, H., & Zhou, Y. 1989, *A&A*, 221, 191
- Bouchet, F. R., Strauss, M. A., Davis, M., Fisher, K. B., Yahil, A., & Huchra, J. P. 1993, *ApJ*, 417, 36
- Butcher, H. & Oemler, A. 1978, *ApJ*, 226, 559
- Caon, N. & Einasto, M. 1995, *MNRAS*, 273, 913
- Capobianco, R. & Renshaw, E. 1998, *Biom. J.*, 40, 431
- Cappi, A., Benoist, C., Da Costa, L., & Maurogordato, S. 1998, *A&A*, 335, 779
- Coleman, P. H. & Pietronero, L. 1992, *Physics Rep.*, 213, 311
- Coles, P. 1993, *MNRAS*, 262, 1065
- Cressie, N. 1991, *Statistics for spatial Data* (Chichester: John Wiley & Sons)
- da Costa, L. N., Willmer, C. N. A., Pellegrini, P., Chaves, O. L., Rite, C., Maia, M. A. G., Geller, M. J., Latham, D. W., Kurtz, M. J., Huchra, J. P., Ramella, M., Fairall, A. P., Smith, C., & Lipari, S. 1998, *AJ*, 116, 1
- Dalton, G., Maddox, S., Sutherland, W., & Efstathiou, G. 1997, *MNRAS*, 289, 263
- Dekel, A. & Lahav, O. 1999, *ApJ*, 520, 24
- Domínguez-Tenreiro, R., Campos, A., Gómez-Flechoso, M. A., & Yepes, G. 1994, *ApJ*, 428, L73
- Domínguez-Tenreiro, R. & Martínez, V. 1989, *ApJ*, 339, L9
- Dressler, A. 1980, *ApJ*, 236, 351
- Dressler, A., Oemler, A., Couch, W. J., Smail, I., Ellis, R. S., Barger, A., Butcher, H., Poggianti, B. M., & Sharples, R. M. 1997, *ApJ*, 490, 577
- Evrard, A., Silk, J., & Szalay, A. 1990, *ApJ*, 365, 13
- Fisher, K. B., Huchra, J. P., Strauss, M. A., Davis, M., Yahil, A., & Schlegel, D. 1995, *ApJS*, 100, 69
- Gardini, A., Bonometto, S., & Macciò, A. 1999, *astro-ph/9911208*

- Geller, M. J. & Beers, T. C. 1982, *PASP*, 94, 421
 Hamilton, A. J. S. 1988, *ApJ*, 331, L59
 Hermit, S., Santiago, B. X., Lahav, O., Strauss, M. A., Davis, M., Dressler, A., & Huchra, J. P. 1996, *MNRAS*, 283, 709
 Isham, V. 1985, in *Spatial Processes and Spatial Time Series Analysis*, ed. F. Droesbeke, Publications des Facultés universitaires Sain-Louis, Bruxelles, 63
 Kaiser, N. 1984, *ApJ*, 284, L9
 Kates, R., Kotok, E., & Klypin, A. 1991, *A&A*, 243, 295
 Kauffmann, G., Nusser, A., & Steinmetz, M. 1997, *MNRAS*, 286, 795
 Kerscher, M. 1998, *A&A*, 336, 29
 —. 1999, *A&A*, 343, 333
 Kerscher, M. 2000, in *Statistical Physics and Spatial Statistics*, ed. K. Mecke & D. Stoyan, *Lecture Notes in Physics* in press (Berlin: Springer Verlag), proceedings of the Conference on Statistical Physics and Spatial Statistics (Wuppertal, Feb. 1999), astro-ph/9912329
 Kerscher, M., Pons-Bordería, M. J., Schmalzing, J., Trasarti-Battistoni, R., Martínez, V. J., Buchert, T., & Valdarnini, R. 1999, *ApJ*, 513, 543
 Lake, G. & Tremaine, S. 1980, *ApJ*, 238, L13
 Maia, M. A. G. & da Costa, L. N. 1990, *ApJ*, 352, 457
 Mann, R. G., Saunders, W., & Taylor, A. N. 1996, *MNRAS*, 279, 636
 Marzke, R., Geller, M., da Costa, L., & Huchra, J. 1995, *AJ*, 110, 477
 Maurogordato, S. & Lachièze-Rey, M. 1987, *ApJ*, 320, 13
 Mecke, K. R., Buchert, T., & Wagner, H. 1994, *A&A*, 288, 697
 Ostriker, J. P. & Turner, E. L. 1979, *ApJ*, 234, 785
 Postman, M. and Geller, M. J. 1984, *ApJ*, 281, 95
 Peebles, P. J. E. 1980, *The Large Scale Structure of the Universe* (Princeton, New Jersey: Princeton University Press)
 Saunders, W., Sutherland, W., Maddox, S., Keeble, O., Oliver, S., Rowan-Robinson, M., McMahon, R., Efstathiou, G., Tadros, H., White, S., Frenk, C., Carraminana, A., & Hawkins, M. 2000, *MNRAS* submitted: astro-ph/0001117
 Schlather, M. 1999, Bernoulli, submitted
 Stoyan, D. 1984, *Math. Nachr.*, 116, 197
 Stoyan, D., Kendall, W. S., & Mecke, J. 1995, *Stochastic Geometry and its Applications*, 2nd edn. (Chichester: John Wiley & Sons)
 Stoyan, D. & Stoyan, H. 1994, *Fractals, Random Shapes and Point Fields* (Chichester: John Wiley & Sons)
 Sylos Labini, F., Montuori, M., & Pietronero, L. 1998, *Physics Rep.*, 293, 61
 Szapudi, I., Branchini, E., Frank, C., & PSCz. 1999, submitted to *MNRAS*
 Tegmark, M. & Bromley, B. C. 1999, *ApJ*, 518, L69
 Valls-Gabaud, D., Alimi, J.-M., & Blanchard, A. 1989, *Nature*, 341, 215
 Valotto, C. A. & Lambas, D. G. 1997, *ApJ*, 481, 594
 van Lieshout, M. N. M. & Baddeley, A. J. 1996, *Statist. Neerlandica*, 50, 344
 —. 1999, *Scandinavian Journal of Statistics*, 26, 511
 Wälder, O. & Stoyan, D. 1996, *Biom. J.*, 38, 895
 Weiß, A. G. & Buchert, T. 1993, *A&A*, 274, 1
 Willmer, C., da Costa, L. N., & Pellegrini, P. 1998, *AJ*, 115, 869

APPENDIX

ESTIMATORS FOR MARK-CORRELATION FUNCTIONS

In this section, we discuss estimators for the weighted mark-correlation functions. For this purpose, let $\{(\mathbf{x}_i, m_i)\}_{i=1}^N$ denote the N empirical data points \mathbf{x}_i inside the sample \mathcal{D} with their marks m_i . We prefer estimators which are unbiased and show small variances. For a detailed discussion of two-point estimators see (Kerscher 1999). One basic idea is to construct estimators for $\langle f \rangle_{\mathcal{P}}(r)$ from a combination of estimators for the numerator and for the denominator of eq. (13). We first discuss estimators of this type, but then introduce a different estimator, which does not use any boundary conditions. It turns out, that in our case, this estimator is unbiased and is recommended by its simplicity and low variance.

Construction of the estimators

To calculate the correlation functions in bins of width Δ , we use the indicator function of a set A

$$\mathbb{1}_A(x) = \begin{cases} 1 & \text{if } x \in A \\ 0 & \text{otherwise,} \end{cases} \quad (\text{A1})$$

and the reduced sample window $\mathcal{D}_{-r} = \{\mathbf{x} \in \mathcal{D} | d(\mathbf{x}, \partial\mathcal{D}) > r\}$ shrunken by r .

Using these definitions, the ratio-unbiased minus estimator $\widehat{\langle f \rangle}_{\mathcal{P}}^M(r)$ for the weighting functions $f(m_1, m_2)$ (compare eq. (13)) is simply

$$\widehat{\langle f \rangle}_{\mathcal{P}}^M(r) = \frac{\sum_{i \neq j=1}^N \mathbb{1}_{\mathcal{D}_{-r}}(\mathbf{x}_i) \mathbb{1}_{[r, r+\Delta]}(|\mathbf{x}_i - \mathbf{x}_j|) f(m_1, m_2)}{\sum_{i \neq j=1}^N \mathbb{1}_{\mathcal{D}_{-r}}(\mathbf{x}_i) \mathbb{1}_{[r, r+\Delta]}(|\mathbf{x}_i - \mathbf{x}_j|)}, \quad (\text{A2})$$

where the indicator function $\mathbb{1}_{\mathcal{D}_{-r}}(\mathbf{x}_i)$ assures that the point \mathbf{x}_i is further than r from the boundary (for details see Kerscher 1999).

In the minus estimator the window is effectively shrunken, resulting in an increased variance. On the contrary, the following estimator uses all point pairs $\mathbf{x}_i, \mathbf{x}_j$, however weighted with an geometrical weight $\omega(\mathbf{x}_i, \mathbf{x}_j)$. Such weighting schemes lead to ratio-unbiased estimators for the two-point correlation function (for details see Stoyan et al. 1995). The straight-forward generalization of these concepts results in ratio-unbiased estimators for $\langle f \rangle_{\mathcal{P}}$:

$$\widehat{\langle f \rangle}_{\mathcal{P}}^{\omega}(r) = \frac{\sum_{i \neq j=1}^N \mathbb{1}_{[r, r+\Delta]}(|\mathbf{x}_i - \mathbf{x}_j|) \omega(\mathbf{x}_i, \mathbf{x}_j) f(m_1, m_2)}{\sum_{i \neq j=1}^N \mathbb{1}_{[r, r+\Delta]}(|\mathbf{x}_i - \mathbf{x}_j|) \omega(\mathbf{x}_i, \mathbf{x}_j)}. \quad (\text{A3})$$

Using the weight

$$\omega(\mathbf{x}_i, \mathbf{x}_j) = \frac{|\mathcal{D}|}{|\mathcal{D} \cap \mathcal{D}_{\mathbf{x}_i - \mathbf{x}_j}|}, \quad (\text{A4})$$

we arrive at an estimator $\widehat{\langle f \rangle}_{\mathcal{P}}^{\omega}(r)$ suggested by Stoyan & Stoyan (1994). In full analogy to the estimators for the two-point correlation function other weights, like the Ripley (Rivolo) weight or the isotropized version of eq. (A4), can be used (for details see Kerscher (1999)).

Instead of estimating $\langle f \rangle_{\text{P}}$ with unbiased estimators for the numerator and for the denominator in Eq. (13) separately, we suggest to simply use the ratio

$$\widehat{\langle f \rangle}_{\text{P}}(r) = \frac{\sum_{i \neq j=1}^N \mathbb{1}_{[r, r+\Delta]}(|\mathbf{x}_i - \mathbf{x}_j|) f(m_1, m_2)}{\sum_{i \neq j=1}^N \mathbb{1}_{[r, r+\Delta]}(|\mathbf{x}_i - \mathbf{x}_j|)}. \quad (\text{A5})$$

This is motivated by the observation, that $\langle f \rangle_{\text{P}}$ is calculated from the marks under the *condition* that the two points are separated by r . Indeed we are not investigating the spatial distribution of the points, but “divide spatial two-point properties out”. Unfortunately, the unbiasedness of this estimator cannot be proven with the common methods used in the theory of point processes, but it seems intuitively clear that this estimator is unbiased. In sect. A.2 we show this using a numerical example; we illustrate furthermore that this estimator has preferable variance properties (this was also observed by Capobianco & Renshaw 1998).

Comparison of the estimators

We use the marked Poisson process discussed in Sect. 3.2 to numerically investigate the properties of these estimators for the continuous mark–correlation functions. The sample mean of the estimators coincide with the theoretical mean value for all estimators. Thus, empirically, all estimators are unbiased. In Fig. A13 the variances of $\gamma(r)/V$ for the different estimators are shown. The variance of the minus estimator becomes unacceptably large especially on large scales. The estimators using a weighting with the set covariance or the isotropized set covariance show the same small variance, even smaller than the variance of the estimator using a weighting of Rivolo (Ripley) type. A detailed inspection shows, that the estimator using no boundary correction typically gives the smallest variance. A qualitatively similar behavior is found for the other mark–correlation functions. Therefore, and for reasons of computational simplicity, we mainly apply this estimator. We suggest to use it for all mark–weighted correlation functions as the natural and unbiased choice.

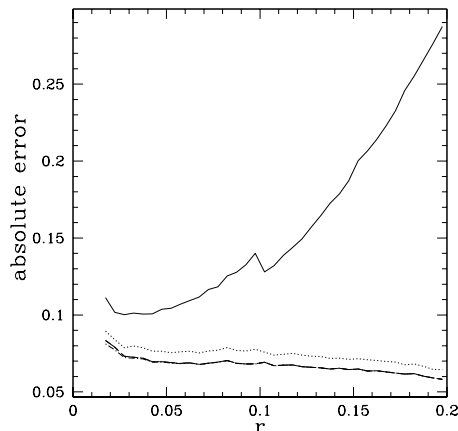


FIG. A13.— The standard error estimated from 5000 realizations for the $\gamma(r)/V$ is shown: minus estimator (solid line), Rivolo (Ripley) estimator (dotted line), the other weighting estimators and the estimator without boundary correction lie nearly on top of each other (the lowest line).